Asian Journal of Chemistry; Vol. 27, No. 3 (2015), 1138-1142

ASIAN JOURNAL OF CHEMISTRY

http://dx.doi.org/10.14233/ajchem.2015.18641

Sol-Gel Method for Preparation of Nanosize $NiFe_{2-x}Co_xO_4$ Using Egg White

RUDY SITUMEANG[1,*], POSMAN MANURUNG[2], SEPTHIAN TRY SULISTIYO[1], SUTOPO HADI[1,*], WASINTON SIMANJUNTAK[1] and SIMON SEMBIRING[2]

[1]Department of Chemistry, FMIPA University of Lampung, Jl. S. Brodjonegoro No. 1 Bandar Lampung 35415, Indonesia
[2]Department of Physics, FMIPA University of Lampung, Jl. S. Brodjonegoro No. 1 Bandar Lampung 35415, Indonesia

*Corresponding authors: E-mail: situmeang@unila.ac.id, sutopo.hadi@fmipa.unila.ac.id

Received: 26 August 2014; *Accepted*: 5 November 2014; *Published online*: 19 January 2015; AJC-16742

$NiCo_xFe_{2-x}O_4$ nanomaterials (with x = 0.1-0.3) have been prepared using a combination method of sol-gel and freeze-drying. Preparation of material was carried out by dissolving nitrate salts of iron, nickel and cobalt in egg white solution and then the sample was stirred throughly using magnetic stirrer. The sample was subjected to calcination treatment and subsequently characterized using the techniques of X-ray diffraction for both qualitative and quantitative analysis such as Rietveld and Debye-Scherrer methods, infrared spectroscopy and scanning electron microscopy. The results of X-ray diffraction characterization indicated that the catalysts consist of various crystalline phases, with $NiFe_2O_4$ superimposed to $CoFe_2O_4$ is a major phase. FTIR analysis confirmed the existence of both Lewis acid and Brønsted-Lowry acid sites. The sample was found to display relatively surface morphology and according to the scanning electron microscopy data and Scherrer equation, the particle size of the material is in nano scale, 15-46 nm.

Keywords: Nanomaterial, Sol-gel and freeze-drying, Brønsted-Lowry and Lewis acid sites.

INTRODUCTION

In the field of material science, development of nanomaterials is the main interest currently pursued intensively since nanomaterial has been proved to posses beneficial characteristics compared to the material with larger particle size, such as higher homogeneity and larger surface area which increase the availability of the active sites. Due to superior performance, many nanomaterials have been developed and applied in wide range of applications, such as catalysts[1,2], sensors[3,4], soft magnetic materials[5,6], microwave absorbers[7,8], colour imaging[9,10] and inductors[11,12].

In recognition of important roles of nanomaterial, a large number of researches has been devoted and focused on two main aspects, *e.g.* development of synthetic method and development of various materials which satisfy the continuous growing of utilization. Currently, several methods for preparation of nanomaterial exist, including co-precipitation[13,14], sol-gel[15,16], soft mechano-chemical[17], hydrothermal[18,19] and precipitation[20,21].

Among the methods mentioned above, sol-gel technique is the most widely applied since this method is acknowledged to offer several advantages in terms of the processing and the characteristics of the product resulted. Sol-gel process can be carried out at ambient temperature using simple apparatus. In addition, since the sol-gel method involves dissolved substrates, the mixing of the substrate in atomic or molecular level can be achieved, resulted in very homogeneous product.

Some researchers have reported succesfull preparation of nanomaterials belong to ferrites compounds using different methods. Derakshi *et al.*[14] reported application of co-precipitation method to synthesize ferrites material with the particle size of 32 nm. In another study[15], it was reported that ferrites material with the particle size of 45 nm was obtained using sol-gel method, followed by sintering treatment at temperature range of 900-1200 °C, while Lazarevic *et al.*[17] applied soft mechanochemical method to obtain ferrites material with particle size of 40 nm.

Recently, global consideration on green chemistry, the material researchers have changed their ideas to use all chemicals on preparing material stuffs which is both amenable to environment and economically reasonable products without diminishing its characteristics[22,23]. Maensiri *et al.*[22] have been able to obtain nano-particle of $NiFe_2O_4$ spinel using ovalbumin solution as non-toxic and economical chemical even the particle size still varied in the range of 60-600 nm. Another study on preparing CeO_2 using egg-white solution, Maensiri *et al.*[23] was able to synthesize plate like clusters of CeO_2 which has the particle size of 6-30 nm in diameter[23]. Other researchers[24,25] have also been able to obtain nanomaterial by using freeze-drying method due to evaporating its solvent without destructing the formed network.

In this paper, we report our result in order to obtain nano-catalysts of $NiFe_{2-x}Co_xO_4$ (x = 0.1-0.3) using freshly egg white solution as capping agent and freeze-drying due to both eliminating its solvent and preventing the precursors' network formed and also to inform the effect of Ni/Co ratio on its characteristics.

EXPERIMENTAL

Catalysts preparation: Solid $NiCo_xFe_{2-x}O_4$ was prepared by dissolving solution of $Fe(NO_3)_3{\cdot}9H_2O$, $Co(NO_3)_3{\cdot}6H_2O$ and $Ni(NO_3)_3{\cdot}6H_2O$, respectively in 100 mL egg white solution. Then, these solutions (by Fe/Co ratio variation, x = 0.1 to 0.3) were mixed and stirred, until homogenous solution is obtained and then freeze-dried. Furthermore, the precursor was calcined at 600 °C for 6 h (increased by 2 °C min^{-1}).

Catalysts characterizations: A small amount of catalyst's sample (50-100 mg) was prepared and put it on sample holder. X-rays power diffraction pattern of $NiCo_xFe_{2-x}O_4$ were recorded from 2θ = 10 to 90° on a Philips diffractometer Model PW 1710 using CuK_α radiation at a step 0.02° per second. Diffractogram then analyzed qualitatively by comparing to ICCD-JCPD files and quantitatively by using Rietveld method[26]. Particle sizes is also determined using Debye-Scherrer method[27].

Scanning electron microscopy analysis: 0.1 g of catalyst's sample is put on sample holder containing Cu sticking tape, then sample is coated by thin layer of gold or other conducting materials[28,29].

Acid sites analysis of catalyst: After heating on 120 °C, sample is inserted in vaccum[30]. Then, liquid pyridine is fluidized into crucible located inside of vaccumized dessicator. After contacting for 24 h, catalyst's sample is taken out from dessicator and allowed on air for 2 h. Finally, a small amount of sample is mixed to KBr powder (sample/KBr ratio = 1/9) and is ready to analyze by putting it on quartz cell of FTIR spectroscopy[31,32].

RESULTS AND DISCUSSION

Acidity analysis: In this study, Fourier transform infrared (FTIR) spectroscopy was applied to identify the functional groups present in the sample. With the main interest is the existence of Brønsted-Lowry and Lewis acid sites, since the acidity is acknowledged as a prime characteristic which determines the performance of a material, for example the catalytic activity. The application of this spectroscopic technique in this study and interpretation of the spectra produced were based on similar studies on various catalyst samples reported by others[33-35]. The FTIR spectra obtained for the three samples investigated are presented in Fig. 1. The spectra are practically similar in terms of the absorption bands, with only some minor differences in the relative intensities of some bands, depending on the composition of the sample. The band at 3385.06, 3379.28 and 3373.49 cm^{-1} of $NiCo_{0,}{}_1Fe_{1,9}O_4$, $NiCo_{0,2}Fe_{1,8}O_4$ and $NiCo_{0,3}Fe_{1,7}O_4$ materials respectively refers to O-H stretching vibration which is usually happened at the range of 3500-3200 cm^{-1}. It can be implied that wavenumber of O-H stretching vibration shifted to the relatively lower band with increasing Co-content. In finger print region, peaks appeared at 586.36, 613.36 and 586.36 cm^{-1} for $NiCo_{0,1}Fe_{1,9}O_4$, $NiCo_{0,2}Fe_{1,8}O_4$ and $NiCo_{0,3}Fe_{1,7}O_4$ materials, respectively which is indicating that stretching vibration of M ↔ O types such as Co ↔ O, Fe ↔ O and Ni ↔ O modes occured. Other peaks represent bending vibration of M ↔ O types such as Co ↔ O, Fe ↔ O and Ni ↔ O modes appeared at 563.21, 567.07 and 561.28 cm^{-1} for $NiCo_{0.1}Fe_{1.9}O_4$, $NiCo_{0.2}Fe_{1.8}O_4$ and $NiCo_{0.3}Fe_{1.7}O_4$ materials, respectively[17,36,37]. In general, stretching vibration happened in a range of 613-580 and at 428-420 cm^{-1} is catagorized as strong or weak stretching vibrations, respectively[38]. So, it can be stated that metal in $NiCo_xFe_{2-x}O_4$ spinel structure is located on tetrahedral sites. The existence of Brønsted-Lowry acid sites is displayed by the absorption bands located both at 1469.75, 1473.61 and 1469.75 cm^{-1} and also at 1421.53, 1436.96 and 1421.53 cm^{-1}, for $NiCo_{0.1}Fe_{1.9}O_4$, $NiCo_{0.2}Fe_{1.8}O_4$ and $NiCo_{0.3}Fe_{1.7}O_4$ materials, respectively. While the existence of Lewis acid site is displayed by the absorption bands located both at 1616.34, 1608.63 and 1612.49 cm^{-1} and also at 1516.05, 1527.62 and 1521.83 cm^{-1} 33,39. Based on the relative intensities of the bands and wavelength locations, it can be inferred that the Lewis acid sites is more prominent than Brønsted-Lowry acid sites. According to this acidity type, it can be inferred that the samples investigated are suitable for process requiring both Lewis and Brønsted-Lowry acid sites, such as dehydrogenation, Fischer-Tropsch, deNO_x and other catalytic reactions[39].

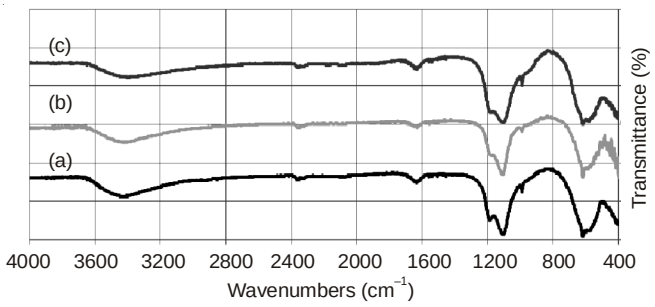

Fig. 1. FTIR spectra of pyridine absorbed on three samples with different compositions investigated in this study, (a) $NiCo_{0,1}Fe_{1,9}O_4$, (b) $NiCo_{0,2}Fe_{1,8}O_4$, and (c) $NiCo_{0,3}Fe_{1,7}O_4$

Characterization using scanning electron microscopy analysis: It is well acknowledged that surface characteristic is an important factor to determine the performance of solid material in the process involving the surface, such as catalytic reaction. In this respect, the samples investigated in this study were characterized using scanning electron microscopy analysis technique and the scanning electron microscopy analysis images obtained are shown in Fig. 2.

As can be seen from Fig. 2, SEM images demonstrated that the surface morphology of the samples are quite different, suggesting the effect of composition. In micrograph (a) shows that the $NiFe_{1.9}Co_{0.1}O_4$ sample has an intact structure, marked by contiguous and smooth surface and also has a cubic structure (Fig. 2a). These cubic structures were well distributed. So it can be said the cubic grains were homogeneous formed. The other samples, $NiFe_{1.8}Co_{0.2}O_4$ and $NiFe_{1.7}Co_{0.3}O_4$, on the other hands, display disrupted surface structure, transforming the surface into porous structure characterized by the existence spherical grains and having agglomeration in to some extent.

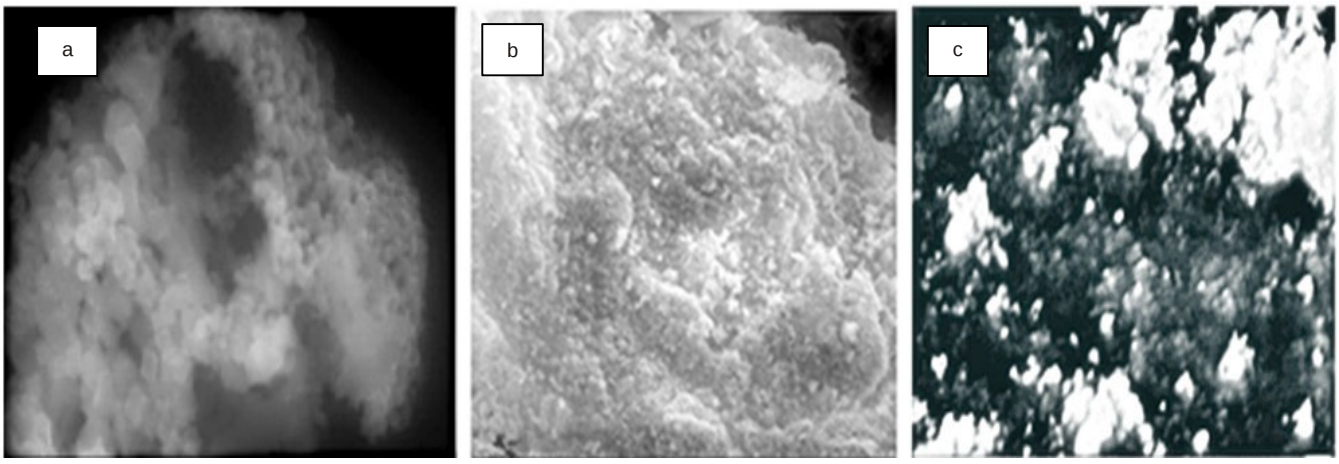

Fig. 2. SEM images of $NiFe_{2-x}Co_xO_4$ samples investigated; (a) x = 0.1, (b) x = 0.2, and (c) x = 0.3

A porous structure increases the surface area accessible to acid sites of material, leading to increased probability of acid-base reaction occured. It is then expected that freeze-drying will facilitate the formation of porous structures. Since micrographs of those samples display cubic grains which are minimal consisted of a couple cubic particle so it is hard to measure and determine definitely its particle size using scanning electron microscopy. Furthermore, the particle size of $NiFe_{2-x}Co_xO_4$ is determined by using Debye-Scherrer equation to difractogram-data representing the main peak of spinel structure[27].

X-Ray diffraction analysis: To investigate the crystalline nature of the samples, the X-ray characterization was carried out and identification of the peaks in diffractograms was carried out qualitatively by comparing the diffraction lines of the samples with those in standard from The powder diffraction files[40]. X-ray diffraction analysis showed that the major phase obtained for the sample isspinel $NiFe_2O_4$(PDF-10-0325) and spinel $CoFe_2O_4$(PDF-22-1086). The X-ray diffractograms for the samples, together with some standards related to the predicted phases of the samples are presented in Fig. 3.

Fig. 3 showed that the diffractograms are practically similar, suggesting that the composition has no effect on the crystallinity of the samples. The main phases observed are $NiFe_2O_4$ and $CoFe_2O_4$. However, other crystalline phases are also identified, in such as NiO (JCPD file no. 47-1049) and Ni_2O_3 (JCPD file no. 14-0481) as minor phases. Furthermore, it has to be noted that crystalline phases of $NiFe_2O_4$ and $CoFe_2O_4$ have a similar spinel crystal structure and its peaks is a slightly

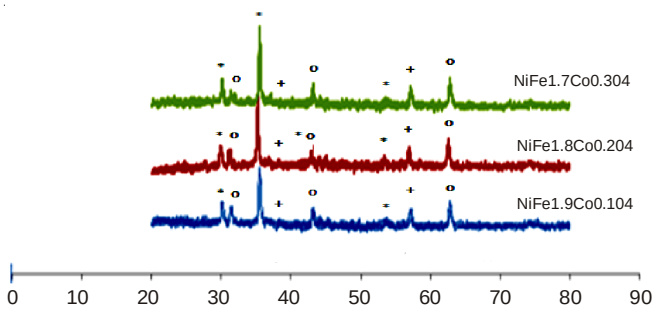

Fig. 3. X-Ray diffractograms of the samples: (a) $NiFe_{1.9}Co_{0.1}O_4$, (b) $NiFe_{1.8}Co_{0.2}O_4$ and (c) $NiFe_{1.7}Co_{0.3}O_4$, with references of $NiFe_2O_4$ and $CoFe_2O_4$ (*), Ni_2O_3(+) and NiO (o) data

different. So it can be implied that both spinel crystalline phase structures are superimposed.

Furthermore, quantitative analysis of $NiFe_{2-x}Co_xO_4$ (x = 0.1-0.3) materials using Rietveld method[26] as shown in Fig. 4, showed that spinel stucture of $M_1M_2Fe_2O_4$ (M_1 = Ni and M_2 = Co_y) is formed with different weight percentage of its crystalline phase obtained and unit cell parameters as shown in Table-1. It can be implied that the relative crystalline phase composition (wt. %) of the sample is affected by the increasing of cobalt content.

However, the maximum crystalline phase of the spinel structure formed was happened on Co/Ni ratio of 0.25. It means that Co - addition into $NiFe_2O_4$ spinel type due to the formation of $NiCo_xFe_{2-x}O_4$ ($A^1A^2B_2O_4$ - type) spinel structure is limited

TABLE-1
RIETVELD REFINEMENT RESULTS OF $NiFe_{2-x}Co_xO_4$(x = 0.1-0.3)

No.	$NiFe_{2-x}Co_xO_4$	Unit cell parameter					Crystal system	Weight (%) $NiFe_{2-x}Co_xO_4$
		a(Å)	b(Å)	c(Å)	V(Å^3)	χ^2		
1	$NiFe_{1.9}Co_{0.1}O_4$	8.354	8.354	8.354	583.02	0.765	Cubic	67.4
2	$NiFe_{1.8}Co_{0.2}O_4$	8.354	8.354	8.354	583.03	0.847	Cubic	74.7
3	$NiFe_{1.7}Co_{0.3}O_4$	8,349	8,349	8,349	582.11	0.699	Cubic	63.3

TABLE-2
PARTICLE SIZE CALCULATION USING DEBYE–SCHERRER EQUATION

Catalyst	2θ (°)	hkl	FWHM (β), radian	Size of particle (D) (nm)
$NiFe_{1.9}Co_{0.1}O_4$	35.5	311	0.00326	44.8
$NiFe_{1.8}Co_{0.2}O_4$	35.2	311	0.00605	24.1
$NiFe_{1.7}Co_{0.3}O_4$	35.46	311	0.00942	15.5

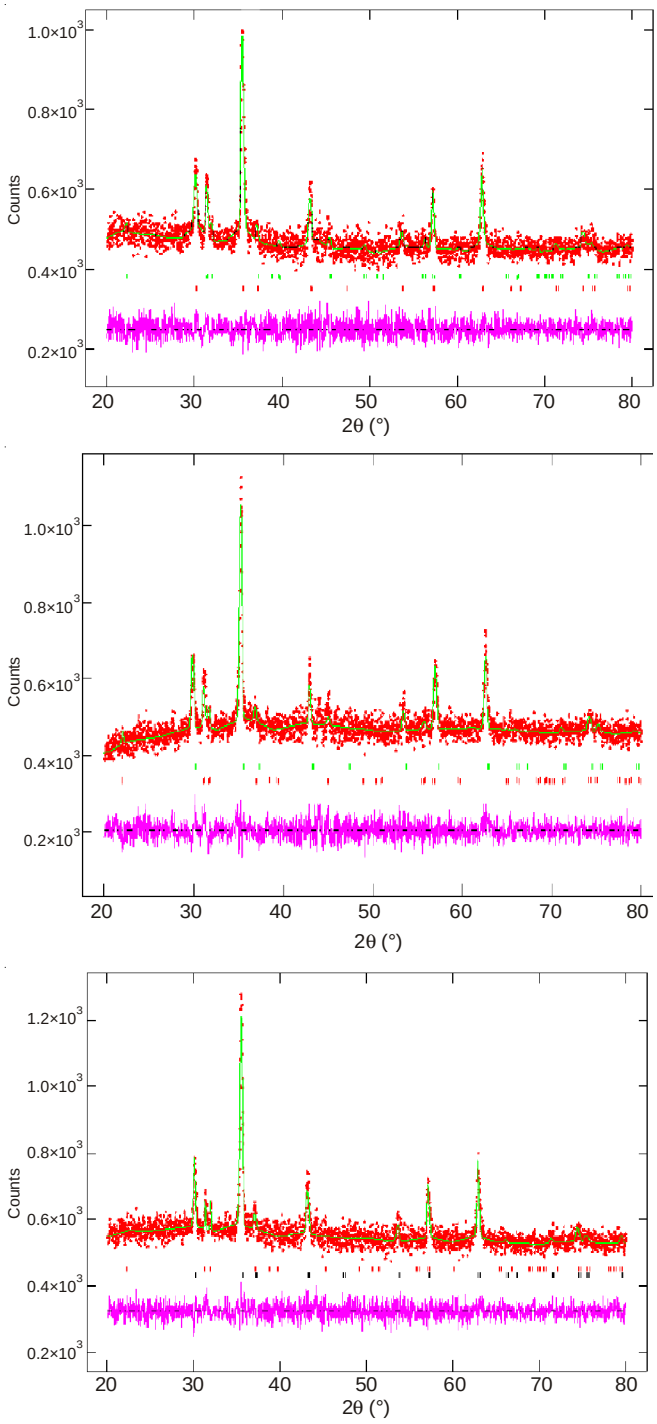

Fig. 4. Result quantitative analysis of $NiFe_{2-y}Co_yO_4$ (y = 0.1-0.3) diffractograms fitted using Rietveld method. The observed data are shown by the (+) red sign, and the calculated data is shown by a solid green line. The purple line (below) is the difference profile between observed and calculated data. The vertical lines (green and red) refers to point series of hkl

by Co/Ni ratio in this condition of preparation. This fact is clearly supported by its cell volume as shown in Table-2 and its density which is 5.240, 5.130 and 5.663 g cm^{-3}, respectively. Consequently, wt. % of other crystalline phases formed which is oxides of nickel (Ni_2O_3) and NiO as a minor phases was also varied.

The particle size of $NiFe_{2-x}Co_xO_4$ (x = 0.1-0.3) was calculated from the full width at half maximum (FWHM) of the representative peak which is a strongest reflection crystalline phase of using the well-known Scherrer formula[27]:

$$D = k \lambda/\beta \cos \theta$$

where D is the crystallite size (nm), k is a constant with a range of 0.9-1.0, lis the X-ray wavelength of CuK_α = 0.154 nm, β is the broadening of diffraction line measured at half maximum intensity (radian) and q is the Bragg's angle in degrees unit. The results are shown in Table-2.

Conclusion

Using egg white solution and freeze drying method is convinient for the synthesis of nano sized Ni-Co ferrites. X-ray diffraction pattern confirm that crystalline phase of spinel Ni-Co ferrites is obtained as much as 75 % at 600 °C. Particle sizes of 15-45 nm were obtained by using Debye-Scherrer calculation. The grain of nano sized Ni-Co ferrites particles is well distributed and homogeneous as confirmed by SEM analyse. FTIR spectra showed that the obtained Ni-Co ferrites materials have Brønsted-Lowry and Lewis acid characteristics as required to catalysis application. The Ni/Co content affected the formation of crystalline phase of Ni-Co ferrites. Furthermore, this simple, relatively low temperature preparation and environmentally friendly method is a good alternative to obtain nano sized of spinel Ni-Co ferrites.

ACKNOWLEDGEMENTS

The authors thank and appreciate the Directorate General Higher Education Republic of Indonesia for research funding provided through The National Grant for Competitive Research University of Lampung and Ministry of Indonesia Higher Education program under contract No. 287/H26/PL/2013.

REFERENCES

1. C.A.G. Fajardo, D. Niznansky, Y. N'Guyen, C. Courson and A.-C. Roger, *Catal. Comm.*, **9**, 864 (2008).
2. V.M. Irurzun, Y. Tan and D.E. Resasco, *Chem. Mater.*, **21**, 2238 (2009).
3. T. Ates, C. Tatar and F. Yakuphanoglu, *Sens. Actuators A*, **190**, 153 (2013).
4. A.M. Soleimanpour and A.H. Jayatissa, *Mater. Sci. Eng. C*, **32**, 2230 (2012).
5. J. Xu, H. Yang, W. Fu, K. Du, Y. Sui, J. Chen, Y. Zeng, M. Li and G. Zou, *J. Magn. Magn. Mater.*, **309**, 307 (2007).
6. S. Wu, A. Sun, W. Xu, Q. Zhang, F. Zhai, P. Logan and A.A. Volinsky, *J. Magn. Magn. Mater.*, **324**, 3899 (2012).
7. A. Sharbati, J.M.V. Khani and G.R. Amiri, *Solid State Commun.*, **152**, 199 (2012).
8. Y. Liu, S.C. Wei, Y.J. Wang, H.L. Tian, H. Tong and B.S. Xu, *Phys. Procedia*, **50**, 43 (2013).
9. D. Raoufi and T. Raoufi, *Appl. Surf. Sci.*, **255**, 5812(2009).
10. Z. Zhao, Z. Yang, Y. Hu, J. Li and X. Fan, *Appl. Surf. Sci.*, **276**, 476 (2013).
11. S. Ilican, Y. Caglar and M. Caglar, *J. Optoelectron. Adv. Mater.*, **10**, 2578 (2008).
12. J. Azadmanjiri, H.K. Salehani, M.R. Barati and F. Farzan, *Mater. Lett.*, **61**, 84 (2007).
13. Y.L.N. Murthy, I.V. KasiViswanath, T. Kondala Rao and R. Singh, *Int. J. Chem. Tech. Res.*, **1**, 1308 (2009).
14. P. Derakhshi, S.A. Khorrami and R. Lotfi, *World Appl. Sci. J.*, **16**, 156 (2012).
15. S. Singhal, J. Singh, S.K. Barthwal and K. Chandra, *J. Solid State Chem.*, **178**, 3183 (2005).
16. W. Trisunaryanti and H.S. Oktaviano, *Indo. J. Chem.*, **8**, 47 (2008).
17. Z.Z. Lazrevic, C. Jovalekic, A. Milutinovic, M.J. Romcevic and N.Z. Romcevic, *Acta Phys. Pol. A*, **121**, 682 (2012).
18. K. Nejati and R. Zabihi, *Chem. Cent. J.*, **6**, 23 (2012).

19. M.G. Naseri, E.B. Saion, H.A. Ahangar, M. Hashim and A.H. Shaari, *Powder Technol*., **212**, 80 (2011).
20. N. Yongvanich, P. Visuttipitukkul, P. Leksuma, V. Vutcharaammat and P. Sangwanpant, *J. Metals Mater. Min*., **20**, 67 (2010).
21. M. Sarkari, F. Fazlollahib, H. Atashi, A.A. Mirzaeid and W.C. Hecker, *Chem. Biochem. Eng. Q*, **27**, 259 (2013).
22. S. Maensiri, C. Masingboon, B. Boonchom and S. Seraphin, *Scr. Mater*., **56**, 797 (2007).
23. S. Maensiri, C. Masingboon, P. Laokul, W. Jareonboon, V. Promarak, P.L. Anderson and S. Seraphin, *Cryst. Growth Des*., **7**, 950 (2007).
24. Y. Peng, D.J. Gardner and Y. Han, *Cellullose*, **19**, 91 (2012).
25. A. Samimi and M. Ghadiri, *Iran. J. Chem. Chem. Eng*., **27**, 69 (2007).
26. H.M. Rietveld, *J. Appl. Cryst*., **2**, 65 (1969).
27. B.D. Cullity, Elements of X-ray Diffraction, Addison-Wesley, London, edn 2, p. 102 (1978).
28. J. Drbohlavova, R. Hrdy, V. Adam, R. Kizek, O. Schneeweiss and J. Hubalek, *Sensors*, **9**, 2352 (2009).
29. L.D. Hanke, Handbook of Analytical Methods for Materials, Materials Evaluation and Engineering Inc. Plymouth, pp. 35-38 (2001).
30. ASTM 4824-13, Test Method for Determination of Catalyst Acidity by Pyridine Chemisorption, MNL 58-EB (2013).
31. E.P. Parry, *J. Catal*., **2**, 371 (1963).
32. A.R. Swoboda and G.W. Kunze, Infrared Study of Pyridine Adsorbed on Montmorillonite Surface. Texas Agricultural Experiment Station, p. 277-288 (2006).
33. M. Yurdakoç, M. Akçay, Y. Tonbul and K. Yurdakoç, *Turk. J. Chem*., **23**, 319 (1999).
34. J. Ryczkowski, *Catal. Today*, **68**, 263 (2001).
35. F. Benaliouche, Y. Boucheffa, P. Ayrault, S. Mignard and P. Magnoux, *Micropor. Macropor. Mater*., **111**, 80 (2008).
36. J.-S. Kim, J.-R. Ahn, C.W. Lee, Y. Murakami and D. Shindo, *J. Mater. Chem*., **11**, 3373 (2001).
37. Z. Wei, H. Qiao, H. Yang, C. Zhang and X. Yan, *J. Alloys Comp*., **479**, 855 (2009).
38. R.M. More, T.J. Shinde, N.D. Choudhari and P.N. Vasambekar, *J. Mater. Sci. Mater. Electron*., **16**, 721 (2005).
39. K. Tanabe, Solid Acids and Bases, Their Catalytic Properties, Kodansha, Tokyo, Academic Press, New York, London, p. 58 (1970).
40. Powder Diffraction File, Diffraction Data for XRD Identification, International Centre for Diffraction Data, PA, USA, (1997).